A Quartic Clough-Tocher Interpolant

Xiang Fang and Stephen Mann
Computer Science, University of Waterloo, 200 University Ave W., Waterloo, Ontario, N2L 3G1, Canada

Keywords: Triangular Bézier Patches, Clough-Tocher Interpolation, Least Squares.

Abstract: In this paper we present a quartic version of the Clough-Tocher scheme for Hermite interpolation of functional data. This variation uses least squares to minimize discontinuities across the macro-patch boundaries, as well as adjusting one of the macro-boundary control points. The resulting surfaces have significantly better shape than a cubic version of Clough-Tocher that also used least squares to minimize discontinuities across patch boundaries. We compare our method to this cubic version of Clough-Tocher using shaded images and Gaussian curvature plots.

1 INTRODUCTION

Scattered data interpolation problems are studied to construct surfaces that interpolate locations and first partial derivatives (normals) at the data sites. Often, the data sites are triangulated and spline construction schemes with Bernstein-Bézier triangular patches are used. The shape of a surface is usually judged by the degree of smoothness. For simple piecewise polynomial surfaces, the minimal degree required to meet C^1 continuity conditions with a single polynomial patch per data triangle is five, and for C^2 continuity the minimum degree is nine (Ženíšek, 1970). These degrees can be reduced by triangle split schemes. One of the simplest schemes is the Clough-Tocher interpolant (Clough and Tocher, 1965), which splits each triangle into three smaller ones. This scheme reduces the degree of C^1 continuous surfaces to three, and also provides an extra degree of freedom for each boundary. Kashyap later gave ways to improve the Clough-Tocher interpolant's quality by adjusting the available degrees of freedom (Kashyap, 1996), and in particular by reducing the discontinuity in the crossboundary derivative.

We present a new scheme to improve the Clough-Tocher interpolant's quality by increasing the order of the surface from three to four. A major limitation of the cubic Clough-Tocher interpolants is that the boundaries of data sites triangles are fixed, which causes wrinkles and bumps. For the quartic version of Clough-Tocher, there is an extra control point on each boundary, which we can set arbitrarily and still interpolate the given data. The interpolant's quality can be improved by adjusting these boundary control points, as well as by reducing the discontinuity in the crossboundary derivatives, where the boundary curve adjustment is based on minimizing the control point movement in the crossboundary adjustment.

The main result of this paper is that the adjustment to the boundary curve in conjunction with a coupled crossboundary adjustment was key to the shape improvements that we obtained. Applying the crossboundary adjustment alone give little or no shape improvements.

We our interested in surface shape, so our primary evaluation of surface quality is visual. Thus while we compute the maximum and root mean square error of the interpolants, we focus on shaded images and Gaussian curvature plots as illustrations of the surface shape and quality.

2 BACKGROUND

In this section, we start with a brief introduction of triangular Bézier patches and continuity between patches (see any CAGD textbook for proofs and additional details (Farin, 2002)).

2.1 Triangular Bézier Patches

A degree n triangular Bézier patch has the form

$$P(t) = \sum_{\vec{i}} P_{\vec{i}} B^n_{\vec{i}}(t)$$

where

$$\vec{i} = (i_0, i_1, i_2) \text{ with } i_0 + i_1 + i_2 = n$$

Fang, X. and Mann, S.
A Quartic Clough-Tocher Interpolant.
DOI: 10.5220/0006547201990206
In *Proceedings of the 13th International Joint Conference on Computer Vision, Imaging and Computer Graphics Theory and Applications (VISIGRAPP 2018) - Volume 1: GRAPP*, pages 199-206
ISBN: 978-989-758-287-5

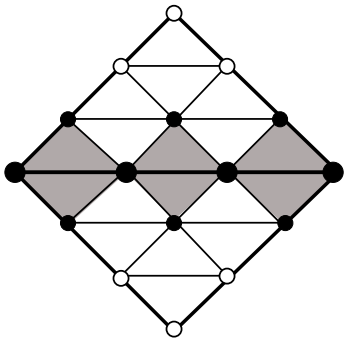

Figure 1: Two patches meet with C^1 continuity if each group of four control points on adjacent (shaded) panels are co-planar.

and $B^n_{\vec{i}}(t)$ are the multi-variate Bernstein polynomials,

$$B^n_{\vec{i}}(t) = \binom{n}{\vec{i}} t_0^{i_0} t_1^{i_1} t_2^{i_2}, \quad \binom{n}{\vec{i}} = \frac{n!}{i_1!i_1!i_2!}$$

and $t = (t_0, t_1, t_2)$ are the barycentric coordinates of the point of evaluation with respect to the domain triangle.

In this paper, we are interested in *functional surfaces* of the form $z = f(x,y)$. In this setting, we can embed the domain in 3-space, and the xy-coordinates of the control points are uniformly distributed over the domain triangle, while the z-coordinates are free to take any values. While the control points are points in 3-space, the xy-coordinates of the control points correspond to points in the embedded domain. At times we will talk about taking the barycentric coordinates of the control points relative to other control points; this should be understood as computing the barycentric coordinates relative to the projection of all these points into the xy-plane.

2.2 Continuity

Our concern in this paper will be with joining patches smoothly, meeting with at least C^1 continuity, although we will also consider C^2 and C^3 continuity. Assume we have two triangular Bézier patches over neighboring triangles, with domains $\triangle CAB$ and $\triangle DBA$. Let (u,v,w) be the barycentric coordinates of D with respect to $\triangle CAB$ and let (u',v',w') be the barycentric coordinates of C with respect to $\triangle DBA$.

The two patches meet with C^0 continuity if they share the same boundary control points (large black points in Figure 1). Two triangular Bézier patches over neighboring triangles meet with C^1 continuity if they meet with C^0 continuity and if adjacent panels are co-planar (Figure 1).

Two triangular Bézier patches meet with C^2 continuity if they meet with C^1 continuity and if we get the same points when the second layer of panels on each side of the boundary are extended using the barycentric coordinates of the corner of one triangle with respect to the other triangle (Lai, 1997). In particular, in the case of cubics (see Figure 2), we require

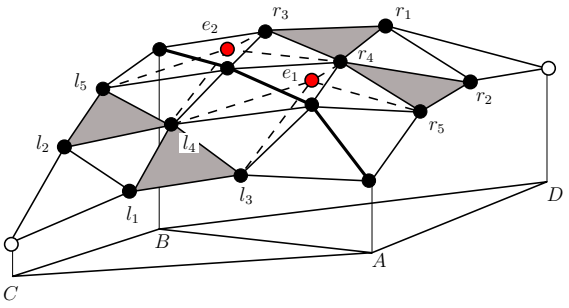

Figure 2: Two patches meet with C^2 continuity if each extensions point (red points) are the same when extending from either patch.

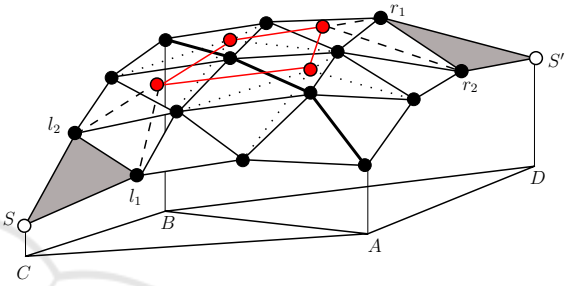

Figure 3: Two patches meet with C^3 continuity if each group of four extension points (red points) are co-planar. The surface interpolates S at C, and the normal to surface at S is perpendicular to the plane spanned by S, l_1, l_2.

$$\begin{aligned} e_1 = ul_1 + vl_3 + wl_4 &= u'r_2 + v'r_4 + w'r_5 \\ e_2 = ul_2 + vl_4 + wl_5 &= u'r_1 + v'r_3 + w'r_4 \end{aligned}$$

Two triangular Bézier patches meet with C^3 continuity if they meet with C^2 continuity and if the extension points of the third layer of panels on each side of the boundary are co-planar with the extension points from the second layer (Lai, 1997). In particular, in the case of cubics (see Figure 3), we require that the points e_1 and e_2 be co-planar with the points

$$uS + vl_1 + wl_2, \qquad u'S' + v'r_1 + w'r_2.$$

Further note that triangular Bézier patches interpolate their corner control points, and that the normal to the surface at the corner of the patch is perpendicular to the plane spanned by the three corner control points (Figure 3).

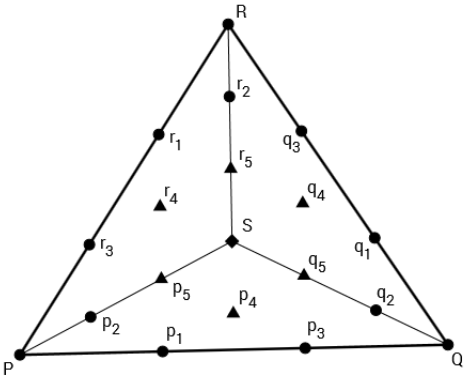

Figure 4: The Clough-Tocher split, showing cubic mini-triangles.

3 CLOUGH-TOCHER INTERPOLANTS

The original Clough-Tocher scheme used cubic Bézier patches. The layout of the control points are shown in Figures 4 and 5. Referring to Figure 4, the original Clough-Tocher scheme had the following steps, with steps 1 and 2 meeting the data interpolation requirements, and steps 3, 4, and 5 meeting the co-planar C^1 continuity requirements:

1. Set P,Q,R to the positional data at the triangle corners.
2. Set r_3, p_2, p_1 to lie in the tangent plane given at vertex P; set p_3, q_2, q_1 to lie in the tangent plane given at vertex Q; set q_3, r_2, r_1 to lie in the tangent plane at R.
3. Set p_4 to be coplanar with p_1, p_3 and the equivalent to p_4 on the other side of the macro-boundary (in Figure 5, this refers to points l_4, c_1, c_2 and r_4 being coplanar); q_4 and r_4 are set in a similar manner.
4. Set p_5 to lie in the plane spanned by p_2, p_4, r_4; q_5 and r_5 are set in a similar manner.
5. Set S to lie in the plane spanned by p_5, q_5, r_5.

The only degree of freedom in this construction is in Step 3 in the settings of the central control points p_4, q_4, and r_4, each of which has a linear degree of freedom. Several algorithms were developed to adjust the central control points to get better shaped interpolants. Two variations of the Clough-Tocher scheme given by Kashyap (Kashyap, 1996) will be reviewed.

3.1 Cubic Precision

One method of improving the quality of the Clough-Tocher interpolant is to set the central control points to achieve cubic precision if position and normal data at a triangle as well as the position data at the three neighboring triangles comes from a cubic; see (Kashyap, 1996; Mann, 1999) for details of the construction.

3.2 Fairing Algorithms

Kashyap used fairing algorithms to improve the shape of the cubic Clough-Tocher interpolant, using both exterior fairing across the macro-boundaries and interior fairing across mini-boundaries. Each operation minimizes or eliminates a specific order of discontinuity while maintaining the conditions of lower order continuity. For the cubic case, we will consider the variation of Kashyap's scheme that starts with the cubic precision Clough-Tocher interpolant, and then adjust the control points to minimize the C^2 discontinuity, while ensuring that the C^1 conditions remained satisfied.

3.2.1 Exterior Fairing

In this section, we give Kashyap's method to update the values of the central control points l_4 and r_4 by minimizing the C^2 discontinuity across the macro-boundaries while maintaining C^1 continuity across the boundary. Figure 5 shows the control points around an exterior boundary. Let (u,v,w) be the barycentric coordinates of S' with respect to $\triangle SP_1P_2$, and let (u',v',w') be the barycentric coordinates of S with respect to $\triangle S'P_2P_1$. The values of l_4 and r_4 need to satisfy the C^1 conditions

$$ul_4 + vc_1 + wc_2 = r_4, \tag{1}$$

and the C^2 discontinuity across the macro-boundary is represented in least squares form as

$$\begin{aligned}&(ul_1 + vl_3 + wl_4 - u'r_2 - v'r_4 - w'r_5)^2 \\ &\quad +(ul_2 + vl_4 + wl_5 - u'r_1 - v'r_3 - w'r_4)^2.\end{aligned} \tag{2}$$

Using least squares to minimize the value of (2) while maintaining condition (1) gives the optimal values of l_4 and r_4 as

$$\begin{aligned} e_1 &= u'r_1 + v'r_3 - ul_2 - wl_5 \\ e_2 &= u'r_2 + w'r_5 - ul_1 - vl_3 \\ e_3 &= 2v^2 + 2w^2 \\ e_4 &= vc_1 + wc_2 \\ l_4 &= (ve_1 + we_2)/e_3 - e_4/2u \\ r_4 &= (uve_1 + uwe_2)/e_3 + e_4/2. \end{aligned} \tag{3}$$

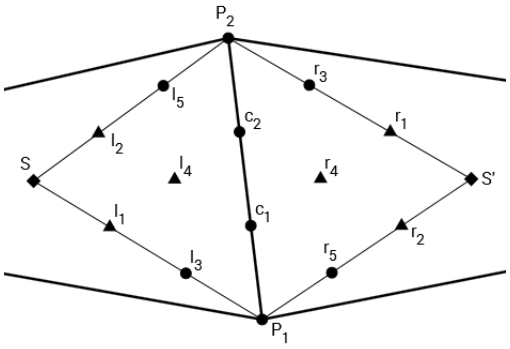

Figure 5: An exterior boundary across cubic macro-triangles.

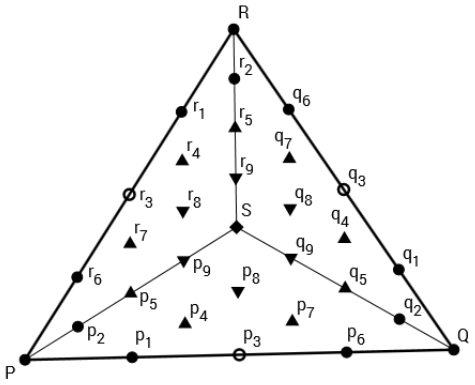

Figure 6: Quartic split triangle.

3.2.2 Interior Fairing

In this section, the surface is smoothed across the mini-triangle boundaries. The method used for minimizing the C^2 discontinuity across exterior boundaries cannot be applied here. Instead, Kashyap forced the control points to satisfy the C^2 continuity conditions, while minimizing the movement of the varying control points from their present location.

Figure 4 shows the control points inside a macro-triangle. To achieve C^2 continuity, the conditions

$$\begin{aligned} E' &= 3p_4 - p_1 - p_3 \\ &= 3q_4 - q_1 - q_3 \\ &= 3r_4 - r_1 - r_3, \end{aligned} \tag{4}$$

where E' is an extension point, must be satisfied. The value of point E' that meets the C^2 condition is not unique, but a unique value can be calculated by minimizing the movement of p_4, q_4, and r_4:

$$(p_4 - \bar{p}_4)^2 + (q_4 - \bar{q}_4)^2 + (r_4 - \bar{r}_4)^2, \tag{5}$$

where $\bar{p}$ is the original value of point p. Then the values of p_4, q_4, and r_4 that minimize the movement of p_4, q_4, and r_4 in a least squares sense are

$$\begin{aligned} E' &= \bar{p}_4 + \bar{q}_4 + \bar{r}_4 \\ &\quad -(p_1 + p_3 + q_1 + q_3 + r_1 + r_3)/3 \\ p_4 &= (S' + p_1 + p_3)/3 \\ q_4 &= (S' + q_1 + q_3)/3 \\ r_4 &= (S' + r_1 + r_3)/3. \end{aligned} \tag{6}$$

3.3 Kashyap's Cubic Scheme

Kashyap's scheme begins by computing the cubic precision Clough-Tocher interpolant. The exterior fairing and interior fairing are then applied repeatedly for a specific amount of times, and finally a C^1 smoothing step is done at the end.

4 QUARTIC CLOUGH-TOCHER INTERPOLANT

In this section, we extend Kashyap's idea for fairing along the macro-boundaries to a quartic Clough-Tocher method. Further, we use the extra freedom of the quartic boundary to adjust the boundary curve to get further shape improvements. Figure 6 shows the control points of the three quartic Bézier patches fit to the three mini-triangles. As a starting point, we again begin with the cubic precision Clough-Tocher interpolant, which we degree raise to get initial positions for the quartic control points. Our fairing methods will adjust the position of these quartic control points.

Although our final algorithm will first adjust the boundary curve and then minimize the crossboundary derivative discontinuity, we present the discontinuity minimization process first, since the boundary curve adjustment is derived from the crossboundary minimization.

4.1 Exterior Fairing

In this section, we perform fairing across the macro-boundaries as a two step process. In the first step, we update the values of the central control points l_7, l_8, r_7 and r_8 to meet all of the C^1 and two of the three C^2 continuity conditions. Then in a second step, we update the values of central control points l_4 and r_4 by minimizing the C^3 discontinuity across the macro-boundary and meet the remaining C^2 continuity condition, while maintaining the C^1 and the first two C^2 continuity conditions.

Figure 7 shows the control points around a exterior boundary. Let (u,v,w) be the barycentric coordinates of S' with respect to $\triangle SP_1P_2$, and let (u',v',w') be the barycentric coordinates of S with respect to

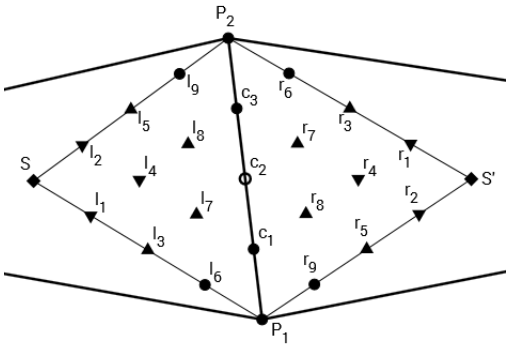

Figure 7: An exterior boundary across quartic macro-triangles.

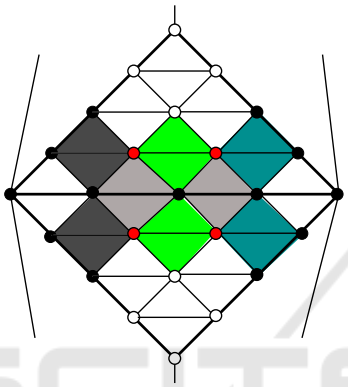

Figure 8: l_7, l_8, r_7, and r_8 (red points) are set to meet the C^1 and C^2 conditions imposed by gray and turquoise panels.

$\triangle S'P_2P_1$. There are three C^2 conditions, as illustrated by the dark gray, green, and turquoise panels in Figure 8. In the first step, we adjust the values of l_7, l_8, r_7 and r_8 to meet the C^1 and two of the C^2 conditions (the ones illustrated by the dark gray and the turquoise panels in Figure 8). The solution to this problem is unique:

$$\begin{array}{rcl} e_1 &=& -u^2l_3 - uvl_6 + r_5 - vr_9 \\ e_2 &=& -u^2l_5 - uwl_9 + r_3 - wr_6 \\ e_3 &=& -vwc_1 - w^2c_2 \\ e_4 &=& -v^2c_2 - vwc_3 \\ l_7 &=& (e_1+e_3)/2uw \\ l_8 &=& (e_2+e_4)/2uv \\ r_7 &=& (e_2-e_4)/2v \\ r_8 &=& (e_1-e_3)/2w. \end{array} \tag{7}$$

In the second step, we adjust the control points l_4 and r_4. The values of l_4 and r_4 (the red points in Figure 9) need to satisfy the conditions

$$ul_4 + vl_7 + wl_8 = u'r_4 + v'r_7 + w'r_8 \tag{8}$$

to meet the third C^2 continuity conditions. The C^3 discontinuity across the macro-boundary can be represented in least squares form as

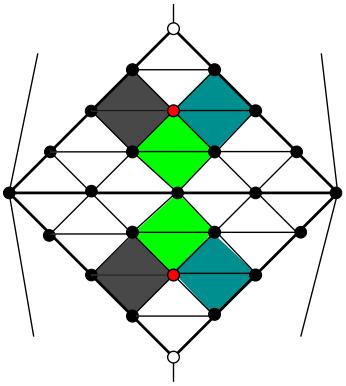

Figure 9: l_4 and r_4 (red points) are set to minimize the C^3 discontinuity (imposed by gray and turquoise panels) while maintaining C^2 condition (green panels).

$$\begin{array}{l} ((u(ul_2+vl_4+wl_5)+vc_2'+wc_3') \\ \quad -(u'r_1+v'r_3+w'r_4))^2 \\ \quad +((u(ul_1+vl_3+wl_4)+vc_1'+wc_2') \\ \quad -(u'r_2+v'r_4+w'r_5))^2 \end{array} \tag{9}$$

where c_1', c_2', and c_3' are the corresponding extension points:

$$\begin{array}{rcl} c_1' &=& ul_3+vl_6+wl_7 \\ &=& u'r_5+v'r_8+w'r_9 \\ c_2' &=& ul_4+vl_7+wl_8 \\ &=& u'r_4+v'r_7+w'r_8 \\ c_3' &=& ul_5+vl_8+wl_9 \\ &=& u'r_3+v'r_6+w'r_7. \end{array} \tag{10}$$

Minimizing the value of (9) in a least squares sense while maintaining condition (8), the optimal values of l_4 and r_4 are

$$\begin{array}{rcl} e_5 &=& u^2l_2+uwl_5+uvw'l_7+uvv'l_8 \\ && -u'r_1-v'r_3 \\ && -ww'r_7-vw'r_8+wa_2 \\ e_6 &=& u^2l_1+uvl_3+uww'l_7+uwv'l_8 \\ && -u'r_2-w'r_5 \\ && -wv'r_7-vv'r_8+va_1 \\ e_7 &=& -(ve_5+we_6)/3(v^2+w^2) \\ l_4 &=& u'e_7+v'l_8+w'l_7 \\ r_4 &=& ue_7+vr_8+wr_7. \end{array} \tag{11}$$

After setting l_7, l_8, r_7, and r_8 with (7) and then setting l_r and r_4 with (11), the patches will meet with C^2 continuity across the macro-patch boundaries (with a minimal C^3 discontinuity), but the patches will meet with only C^0 across mini-patch boundaries.

4.2 Macro-Boundaries Modification

In this section we will adjust the boundary curves along macro-patch boundaries. A quartic boundary

curve has five control points. In our quartic Clough-Tocher scheme, four of the control points on each macro-boundary are set by the position and tangent information that the patch needs to interpolate. This leaves one control point whose value we can adjust to achieve better shape. In particular, we can adjust the value of c_2 in Figure 7. Initially this control point comes from the degree raised cubic precision Clough-Tocher interpolant. With the method described in Section 4.1, for a given value of c_2, there exist a corresponding value of c_2' and a corresponding optimal C^3 discontinuity value across the exterior boundary.

One idea is to treat c_2 as a variable, and substitute the relationship between c_2' and c_2 in Section 4.1 into the formula of C^3 discontinuity (9), then minimize the C^3 discontinuity across the exterior boundary. However, the resulting C^3 discontinuity equation is independent of the value of c_2. Thus this approach cannot be used to adjust the boundary control point c_2.

Instead, we use the approach that Kashyap used on the interior boundaries, and we find the settings of c_2' such that the movement of l_4 and r_4 will be minimized when a variation of the C^3 minimization of (9) is used. We minimize

$$\begin{aligned}&(u'c_2'+v'l_8+w'l_7-\bar{l}_4)^2\\&+(uc_2'+vr_8+wr_7-\bar{r}_4)^2\end{aligned}\tag{12}$$

in a least squares sense, where $\bar{l}_4$ and $\bar{r}_4$ is the original value of points l_4 and r_4. The optimal value of c_2' is

$$\begin{aligned}f_1 &= -u^2l_3-uvl_6+r_5-vr_9\\ f_2 &= -u^2l_5-uwl_9+r_3-wr_6\\ f_3 &= -vwc_1-w^2c_2\\ f_4 &= -v^2c_2-vwc_3\\ c_2' &= (u'\bar{l}_4+u\bar{r}_4-\tfrac{v'}{2v}(f_2+f_4)\\ &\quad -\tfrac{w'}{2w}(f_1+f_3)-\tfrac{uv}{2w}(f_1-f_3)\\ &\quad -\tfrac{uw}{2v}(f_2-f_4))/(u^2+u'^2),\end{aligned}\tag{13}$$

which can be rewritten as

$$\begin{aligned}f_5 &= \Big(u'\bar{l}_4+u\bar{r}_4\\ &\quad -\tfrac{u'w'+u^2v}{2uw}f_1\\ &\quad -\tfrac{u'v'+u^2w}{2uv}f_2\\ &\quad -\tfrac{uv^2+u'w'^2}{2}c_1\\ &\quad -\tfrac{uw^2+u'v'^2}{2}c_3\Big)/(u^2+u'^2)\\ f_6 &= -(uvw+u'v'w')/(u^2+u'^2)\\ c_2' &= f_5+f_6c_2.\end{aligned}\tag{14}$$

With c_2 as the variable, we now perform least squares minimization of (9) using (10) for c_1' and c_3' but (14) for c_2' (Figure 10 illustrates this construction graphically). The least squares minimization gives

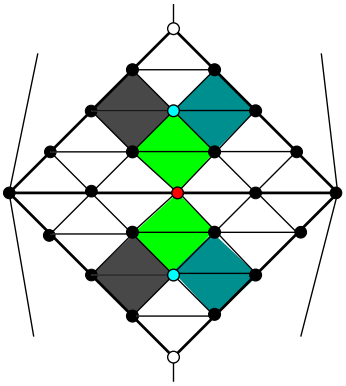

Figure 10: Adjusting the red (boundary) control point to minimize movement of cyan points on the C^3 minimization step.

$$\begin{aligned}f_7 &= u^2l_2+\tfrac{3}{2}uwl_5+\tfrac{1}{2}w^2l_9-u'r_1\\ &\quad -\tfrac{3}{2}v'r_3+\tfrac{1}{2}wv'r_6\\ &\quad -v^2w'c_1-\tfrac{1}{2}w^2w'c_3\\ f_8 &= u^2l_1+\tfrac{3}{2}uvl_3+\tfrac{1}{2}v^2l_6-u'r_2\\ &\quad -\tfrac{3}{2}w'r_5+\tfrac{1}{2}vw'r_9\\ &\quad -\tfrac{1}{2}v^2v'c_1-w^2v'c_3\\ f_9 &= -\tfrac{3}{2}v^2v'\\ f_{10} &= -\tfrac{3}{2}w^2w'\\ f_{11} &= (f_7+3vf_5)(f_9+3vf_6)\\ &\quad +(f_8+3wf_5)(f_{10}+3wf_6)\\ f_{12} &= (f_9+3vf_6)^2+(f_{10}+3wf_6)^2\\ c_2 &= -f_{11}/f_{12}.\end{aligned}\tag{15}$$

Our algorithm will set c_2 with (15) and then apply the macro-boundary optimization of the previous section.

4.3 C^1 Smoothing

After adjusting the interior control points as described in Section 4.1, the mini-patches will only meet with C^0 continuity. We need an additional step, similar to the original Clough-Tocher, to make the patches meet with C^1 continuity across the mini-patch boundaries. Referring to Figure 6, the following constructs a C^1 join across the mini-boundaries of the quartic patch:

1. Set p_5 to lie in the plane spanned by p_2, p_4, r_7; q_5 to lie in the plane spanned by q_2, q_4, p_7; and r_5 to lie in the plane spanned by r_2, r_4, q_7.
2. Set p_9 to lie in the plane spanned by p_5, p_8, r_8; q_9 to lie in the plane spanned by q_5, q_8, p_8; and r_9 to lie in the plane spanned by r_5, r_8, q_8.
3. Finally, set S to lie in the plane spanned by p_9, r_9, q_9.

```
Construct the cubic precision interpolant
for i=0 to N
    Adjust the boundary control points
        Set c2 with (15)
    Exterior Fairing
        Set l7,l8,r7,r8 with (7)
        Set l4,r4 with (11)
    C1 Smoothing (Section 4.3)
end
```

Figure 11: Code for quartic Clough-Tocher algorithm.

Table 1: Comparison of errors.

	Cubic Precision	Kashyap	Quartic
RMS	0.0172	0.0166	0.0170
Max	0.0754	0.0752	0.0690

5 ALGORITHM AND EXAMPLE

Similar to Kashyap's scheme, our algorithm iterates between three adjustments: adjusting the boundary control points (Section 4.2); adjusting the crossboundary control points (Section 4.1); and C^1 smoothing on mini-triangle boundaries (Section 4.3). Pseudo-code for our algorithm appears in Figure 11. The cubic precision Clough-Tocher interpolant was used to create initial locations for the control points of our method as well as the variation of Kashyap's method that we implemented.

Figure 12 compares the error of our method to the cubic precision interpolant and to Kashyap's scheme on a sampling of the Frankye function (Frankye, 1982),

$$\begin{aligned} F(x,y) \;=\; & 0.75e^{-\frac{(9x-2)^2+(9y-2)^2}{4}} \\ & +0.75e^{-\frac{(9x+1)^2}{49}-\frac{9y+1}{10}} \\ & +0.5e^{-\frac{(9x-7)^2+(9y-3)^2}{4}} \\ & -0.2e^{-(9x-4)^2-(9y-7)^2}, \end{aligned}$$

where we used a 5×5 sampling of F as our data. Table 1 gives both the RMS error and the maximum ($|CT-F|$) error for the three methods on this data. From the data, we see that the errors are not substantially different. As our interest is more in shape than in data reproduction, Figure 13 shows shaded images and Gaussian curvature plots of the three surfaces. Here we see that despite similar error, Kashyap's scheme gives a visible improvement over the cubic precision Clough-Tocher interpolant, while our quartic scheme gives a visual improvement over Kashyap's scheme.

6 CONCLUSIONS

In this paper, we presented a quartic version of Clough-Tocher interpolation that gives a shape improvement over a similar cubic scheme of Kashyap. Both methods used least squares to do fairing of the surfaces. However, while Kashyap did fairing across both the macro- and mini-boundaries, we used fairing across the macro-boundaries and to adjust the macro-boundary curve. The adjustment to the macro-boundary curve was key to our shape improvements. We also tested a method to smooth across the mini-triangle boundaries (similar to what Kashyap did, although with our higher degree patches, our mini-triangle smoothing achieved C^3 continuity across the mini-triangle boundaries). However, with this interior smoothing step in the quartic scheme, our quartic surfaces were of similar quality to Kashyap's cubic surfaces. It was only when we adjusted the macro-boundary (and no longer did interior boundary discontinuity minimization) that our quartic scheme gave better surfaces than Kashyap's cubic scheme.

Additional details of our scheme can be found in (Fang, 2017).

REFERENCES

Clough, R. and Tocher, J. (1965). Finite element stiffness matrices for analysis of plates in bending. *Proceedings of the Conference on Matrix Methods in Structural Mechanics*, pages 515–545.

Fang, X. (2017). Using least squares to construct approximate continuous Clough-Tocher interpolant. Master's thesis, University of Waterloo.

Farin, G. (2002). *Curves and Surfaces for CAGD*. Morgan-Kaufmann.

Frankye, R. (1982). Scattered data interpolation: Tests of some methods. *Mathematics of Computation*, 39:181–200.

Kashyap, P. (1996). Improving Clough-Tocher interpolants. *CAGD*, 13(7):629–651.

Lai, M.-J. (1997). Geometric interpretation of smoothness conditions of triangular polynomial patches. *CAGD*, 14(2):191–197.

Mann, S. (1999). Cubic precision Clough-Tocher interpolation. *CAGD*, 16(2):85–88.

Ženíšek, A. (1970). Interpolation polynomials on the triangle. *Numerische Mathematik*, 15:283–296.

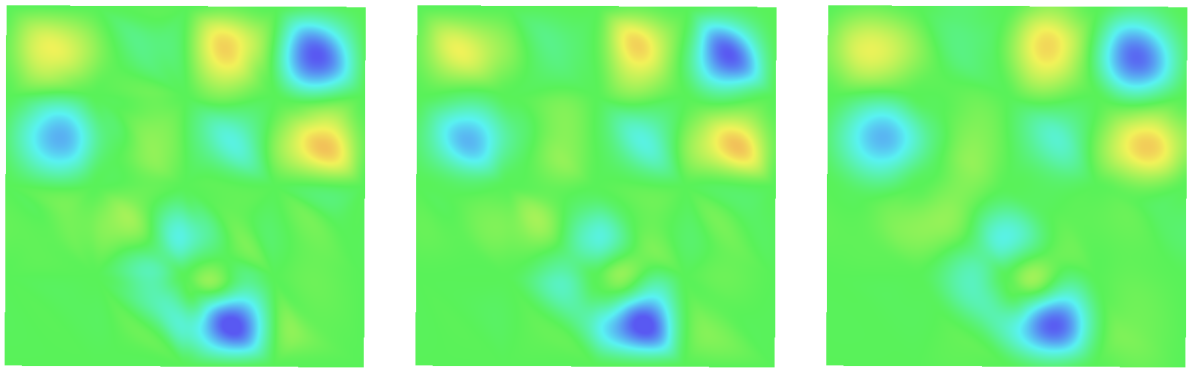

Figure 12: 2D Error Plots. Left: cubic precision; middle: Kashyap's scheme; right: quartic scheme. Blue represents negative error, green represents zero error, yellow/red represent positive error, with error values in the range of $[-0.0754, 0.0436]$.

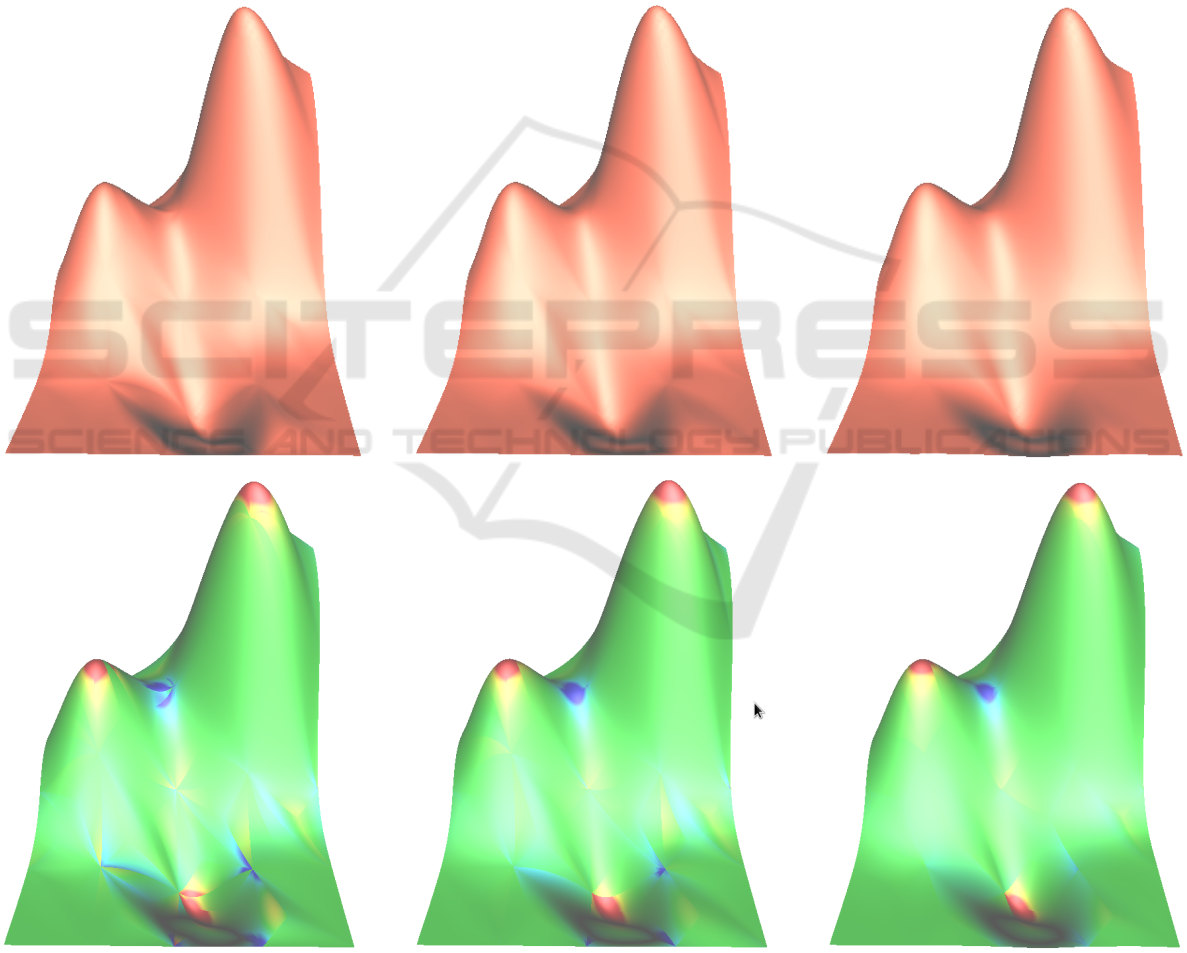

Figure 13: Left: cubic precision; middle: Kashyap's scheme; right: quartic scheme. Top row: shaded images; bottom row: Gaussian curvature plots. Blue represents negative Gaussian curvature, zero represents zero Gaussian curvature, and yellow/red represent positive Gaussian curvature.